Proceedings of Meetings on Acoustics

Volume 19, 2013 http://acousticalsociety.org/

ICA 2013 Montreal
Montreal, Canada
2 - 7 June 2013

Physical Acoustics
Session 3pPAb: General Physical Acoustics II

3pPAb3. Influence of reflecting walls on edge diffraction simulation in geometrical acoustics

Alexander Pohl*, Dirk Schröder, Uwe M. Stephenson and Peter Svensson

***Corresponding author's address: HafenCity University, Hamburg, 22297, Hamburg, Germany, alexander.pohl@hcu-hamburg.de**

Edge diffraction can be introduced into Geometrical Acoustics mainly by three models: detour-based, energetic and wave-based diffraction models. In the past, we thoroughly compared Maekawa's detour law, the uncertainty relation based diffraction method and the secondary source model by the example of edge diffraction of a single wedge. However, the influence of the wedge shape has not yet been analyzed. Therefore, we consequently study in this contribution the influence of the wedge's faces. This is analyzed by varying both the faces' reflection properties and their opening angle. This is extended to the crucial case of approximately parallel faces (inner angle e.g.179°), where diffraction is physically neglectable, but computationally problematic for the uncertainty based diffraction method. Additionally, wedges are placed on an infinitely long surface. Therewith, we can analyze the floor reflections' impact on the sound field behind the wedge by varying both their absorption and scattering coefficients. Furthermore, we discuss artifacts which can arise in the uncertainty based diffraction model due to arbitrary positioning of diffraction planes, so called 'transparent walls'. Finally, we discuss the advantages and disadvantages of the presented methods.

Published by the Acoustical Society of America through the American Institute of Physics

Received 22 Jan 2013; published 2 Jun 2013

INTRODUCTION

In room acoustics and noise immission prognosis (urban acoustics), the methods of Geometrical Acoustics (GA) are well approved. While the Image Source Method (ISM) is a deterministic method that is often combined with a coherent handling of sound, the Sound Particle Simulation Method (SPSM) uses rays or particles to transport sound powers or energies and statistically computes the local energy densities [1]. However, in many practical cases, the SPSM proves to be much more efficient, especially for higher order reflections. The efficient simulation of higher order reflections with diffractions is a general aim of our work[2]. As a matter of principle, however, all native methods of GA neglect the wave effect of diffraction, although it is often a dominant wave propagation effect, especially in outdoor or urban surroundings. While single diffraction at a screen is no problem, effective solutions for higher order diffraction and the generalization to an arbitrary combination with reflections are still missing. For the SPSM, a diffraction module is desired as an approximation for short, but not very short wavelengths.

This paper is devoted mainly to a comparison of a strictly wave theory based Secondary Source Model (SSM) and an energetic sound particle diffraction model that utilizes the Uncertainty Relation-Based Diffraction (URBD). The results for a single screen are additionally compared with the Maekawa Detour Law (MDL). Many basic comparisons have already been performed successfully[3, 4]. So, aiming at the mentioned generalization, some new experiments that combine diffraction with reflections of first order have been performed. The URBD sound particle model takes neither the wedge angle nor the horizontal rotation of the wedge into account. In this contribution, the former aspect is analyzed, but the latter is left for further studies. Therefore, the experiments presented here can use a 2D modeling approach.

A CLASSIFICATION OF THE INVESTIGATED DIFFRACTION MODELS

Among the above mentioned simulation methods of GA, mainly three approaches are used today for edge diffraction calculations – classified here with respect to their degree of approximation and application:

1. Wave theoretical methods that remain in the wave domain, such as the SSM. This is an exact solution for the infinite wedge for single diffraction taking the flanking walls as a boundary condition into account. For higher orders still coherent, it is intended to be combined recursively with the ISM. Unfortunately, these methods are of increased mathematical complexity, which makes them (especially if combined with the inefficient ISM) hardly applicable for edge diffraction calculations of higher order.

2. Energetic methods, intuitively to be combined with sound particles as energy carriers, an approximation model, as further interference effects are neglected, but efficient as the SPSM is a straightforward simulation. The idea is to take only important, i.e., nearby edges into account, while flanking walls are handled by the SPSM separately. These methods consider only the aperture above the edge and assume that the incident sound field is undisturbed (Kirchhoff approximation). Angle dependent ray diffraction functions[5, 6, 1] follow from Fresnel's theory for the half-infinite screen (instead of an extended wedge), and from Fraunhofer's theory for the slit.

3. Simplified methods, also energetic, aiming at computing approximately the screening effect of a (laterally infinitely extended) screen. For this special but most important case, a detour law for small diffraction angles can be derived[5][7] from the Fresnel theory, first found empirically by Maekawa[8]. This is often used in guidelines for noise immission prognosis and noise barriers, and therefore shall serve as a standard and reference here.

The Secondary Source Model (wave-theoretical/coherent)

The theories of Biot-Tolstoy-Medwin (BTM), handle diffraction around an infinite wedge[9] in an exact way taking the boundary condition of the wedge faces into account, but only perfectly rigid, or pressure-release (soft). The main idea of BTM is the introduction of a displacement potential. It is defined such that the boundary conditions of both the wedge faces and the sound source are fulfilled. The sound pressure for an arbitrary receiver within the defined volume is then determined by means of this displacement potential. The overall result is an integral over an infinitely long edge that accumulates the contributions of infinitesimal small edge elements with different delay and attenuation in relation to the respective sound source/receiver position. Based on the BTM theory, Svensson et al.[10] presented a SSM that utilizes secondary sound sources for covering these small edge elements. The method extends the BTM to both curved edges and higher order diffraction. It is exact for first-order diffraction and shows very good results for higher-order diffraction. So far, solutions for the rigid and soft wedge case exist. Svensson's MATLAB Edge Diffraction Toolbox (EDB) is freely available on the internet[11] and enables a handy computation of time domain impulse responses.

The Uncertainty Relation Based Diffraction (energetic/incoherent)

Particles will never hit edges exactly due to their zero-dimensional nature and, therefore, can only pass nearby. Thus, the effective SPSM cannot be combined with exact diffraction models. Inspired by Heisenberg's uncertainty relation, the intuitive idea is that the deflection probability of a sound particle increases with decreasing distance to the edge.

This effect is described by a Deflection Angle Probability Density Function (DAPDF) which is derived from the Fraunhofer diffraction at an imaginary slit, whose width is proportional to the bypass distance and averaged over an octave band[1]. For implementation, it is more efficient (and physically equivalent) to split up the sound particles into secondary ones. The latter are equally distributed and their energy is computed by an integral over the DAPDF. To detect diffraction events near inner edges, Transparent Walls (TWs) are introduced on edges disturbing the convexity, where sound particles are diffracted. Thus, diffraction is computed for wedges with an angle of up to $\varphi_W = 179°$, but not for angles greater than $\varphi_W = 181°$. This is interesting, as the simple uncertainty based model *sees* only the distance to the edge and not to other surfaces nearby such that the results are independent of such a wedge angle.

The DAPDF has been tested in many experiments with a screen and a slit as reference cases[1]. For a better agreement with the SSM, the DAPDF has recently been improved by an attenuating term for large angles (D_3 in[12]).

The Maekawa Detour Law (a single screen approximation, MDL)

Maekawa carried out empirical measurements at a single wedge and showed that diffraction around the edge of a semi-infinite screen is mainly influenced by the sound wave's shortest detour around an obstacle (in units of wavelengths λ). In 1968 he published his famous chart on this [8]). This detour law is, however, only a valid approximation for a single thin screen, and only for one detour path. Furthermore, it is only valid for small diffraction angles resulting in huge discrepancies with the other two models in the deep shadow zone. In order to combine the detour law with floor reflections, the ISM may be used, but often simply $3dB$ is added for each reflecting floor. As a practical, but rough approximation, the second approach is applied.

THE METHOD OF EVALUATION

In the following, the influence of sound reflections (specular or diffuse) on the diffraction process are investigated. Therefore, the previous single wedge experiment[3] is extended by reflecting surfaces, i.e., a certain absorption coefficients α and scattering coefficients σ are assigned to the floor and/or the wedge's faces.

All numerical experiments are used to compute the transmission degree T (and the transmission level $L = 10 \cdot log_{10}(T)$). T is defined as the proportion of the intensity with the diffraction at an obstacle relative to the free-field intensity. This makes the result independent of the source power and, thus, only describes the effect of the obstacle. The described diffraction modules are applied to some typical test cases. In general, the receiver angle is varied and the distances of source and receiver remain constant. These distances are expressed in units of wavelengths λ. Here, a reasonable, medium distance of 10λ is chosen. However, the conclusions made are applicable to other distances, because the influence of the distance is weak compared to the influence of the receiver angle. In the case of very small distances some near field errors occur. Further investigations with a varying source position are pointless due to the fulfilled reciprocity principle. Therefore, the source remains at a fixed position. The EDB computes impulse responses for absolute distances. To use the EDB, the relative distances l are converted to absolute distances by $s = l \cdot \frac{c}{f}$ for an arbitrary frequency of $f = 1000Hz$, where c is the speed of sound. Finally, the impulse responses are averaged over an octave band around f.

In the following examples, the edge is defined as the (infinitely long) $z-axis$, the $x-axis$ is directed to the right and the $y-axis$ points upwards (see Fig. 1). Source and receiver lie in the

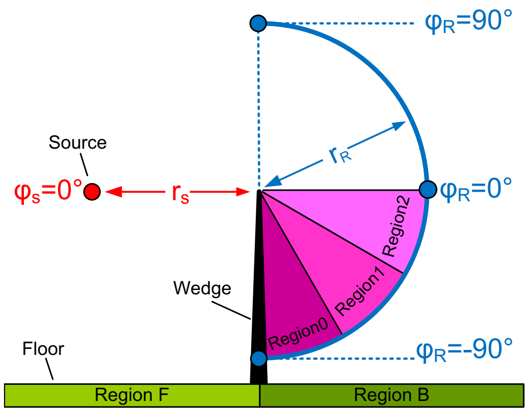

(A) Geometrical setup for the single wedge experiment.

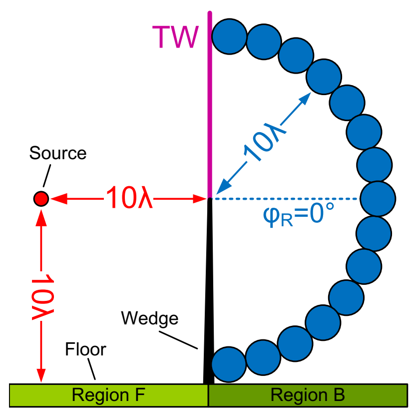

(B) Geometrical setup for the introduction of floor reflections.

FIGURE 1: Single wedge setup.

same $x-y-plane$ with the source at $y = 0 (\varphi_S = 0°)$. 15 receivers are equally distributed in the range of $\varphi_R = -90...+90°$ and their diameters are chosen such that they are tangent to each other. For a better overview and classification, the shadow zone (i.e., receiver angles $-90° < \varphi_R < 0°$ for a source at $\varphi_S = 0°$) is subdivided into three ranges: deep shadow ($-90° < \varphi_R < -60°$,region0), medium shadow ($-60° < \varphi_R < -30°$, region1) and upper shadow zone ($-30°...0°$, region2) (see Fig. 1). The region $0° < \varphi_R < 90°$ is called view zone. The floor is divided into the regions F and B, where F and B denote the floor area in front of and behind the wedge, respectively (see Fig. 1).

As a result of previous numerical experiments and achieved accuracies ($< 0.1dB$), the sound particle simulations were performed with $N = 2000$ primary sound particles and each sound particle splits up into $S = 200$ secondary sound particles on scattering or diffraction events.

EXPERIMENT I: THE EFFECT OF FLOOR REFLECTIONS

The first experiment was designed to investigate the influence of floor reflections on diffraction. The wedge's closed angle is set to 1°. The wedge's faces were defined as rigid for the SSM as it cannot handle completely absorbent wedge surfaces, but remain completely absorbent for the URBD. The floor conditions of region F and/or B were varied by setting them either to full absorbent ($\sigma = 0.0$, $\alpha = 1.0$), rigid ($\sigma = 0.0$, $\alpha = 0.0$) or scattering ($\sigma = 1.0$, $\alpha = 0.0$) resulting in three main simulation series. In case of the SSM, no scattering surfaces were simulated since the EDB could only process specular reflections. All numerical results of this experiment are summarized in Tab. 1.

TABLE 1: Difference in transmission level of different simulations separated by regions. All values are in dB and an average over the region's receivers.

Simulation Series				Shadow Zone Region 0	Shadow Zone Region 1	Shadow Zone Region 2	View Zone	Both Zones
Series 1	Front	MDL	Abs - Rig	-3.0	-3.0	-3.0	-3.0	-3.0
		URBD	Abs - Sca	-0.7	-0.6	-0.3	-0.6	-0.6
			Abs - Rig	-0.7	-0.6	-0.3	-0.5	-0.5
			Rig - Sca	0.0	0.0	0.0	-0.1	-0.1
		SSM	Abs - Rig	-0.7	-0.5	-0.2	-0.3	-0.4
Series 2	Behind	MDL	Abs - Rig	-3.0	-3.0	-3.0	-3.0	-3.0
		URBD	Abs - Sca	-3.7	-2.3	-0.7	0.0	-1.1
			Abs - Rig	-3.3	-1.8	-0.5	0.0	-0.9
			Rig - Sca	-0.4	-0.6	-0.2	0.0	-0.2
		SSM	Abs - Rig	-4.8	-1.8	-0.3	0.0	-1.0
Series 3	Both	MDL	Abs - Rig	-6.0	-6.0	-6.0	-6.0	-6.0
		URBD	Abs - Sca	-4.4	-2.9	-1.0	-0.7	-1.7
			Abs - Rig	-4.0	-2.4	-0.8	-0.5	-1.4
			Rig - Sca	-0.4	-0.5	-0.2	-0.1	-0.3
		SSM	Abs - Rig	-5.0	-2.1	-0.5	-0.3	-1.3

Series 1: The first simulation series focused on the floor in front of the wedge (region F). Therefore, region B was set to completely absorbent and region F was modeled – as described above – either as full absorbent, rigid or scattering.

Shadow Zone: The URBD transmission levels for the rigid and scattering case are slightly higher ($< 0.6dB$) in comparison to the completely absorbent setup (see Fig. 2a and Tab. 1). This can be explained, as the sound particles reflected from the floor have a significantly lower energy due to two effects: the total diffraction angle is larger and the sound particles have to travel a longer distance.

The small difference between the rigid and scattering case is explainable by the fact that the main diffracted energy comes from sound particles that intersect the TW very close to the edge[1]. From a rigid surface (or an image source, respectively), the number of sound particles that can reach that area above the edge is small, whereas in the scattering case the complete region F reflects (secondary) sound particles such that more of them reach the vicinity of the edge - but with reduced energy. The main result is: the SSM computes exactly the same difference for the rigid and the absorbent surface as the URBD.

View Zone: The introduction of either a rigid or a scattering surface increases the transmission level computed with the URBD up to $0.6dB$. In case of the rigid surface, with the proportions given here, this happens at angles of $\varphi_R \approx 63.4°$, because then specular reflected sound particles may reach the receivers (or the image source below the floor becomes visible). This hard transition is *smeared* in the case of a scattering floor. The SSM shows the same behavior like the URBD with a rigid surface, but the increase of transmission levels is smaller.

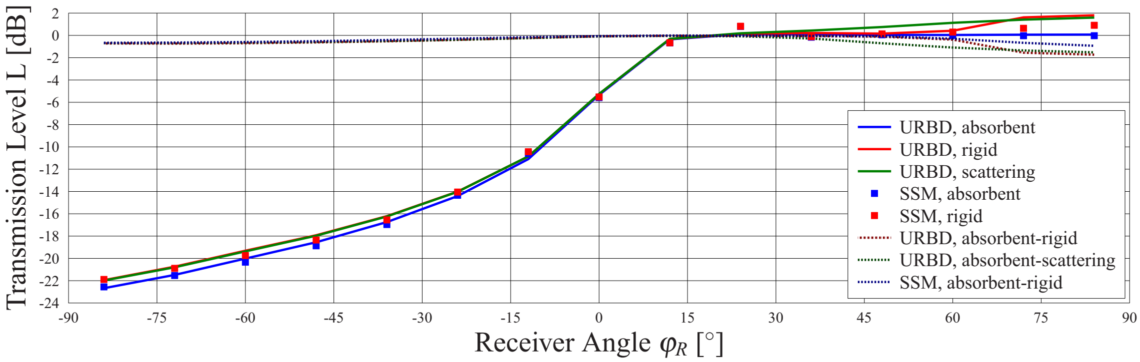

(A) Reflecting surface in front of the wedge, either specular or diffuse.

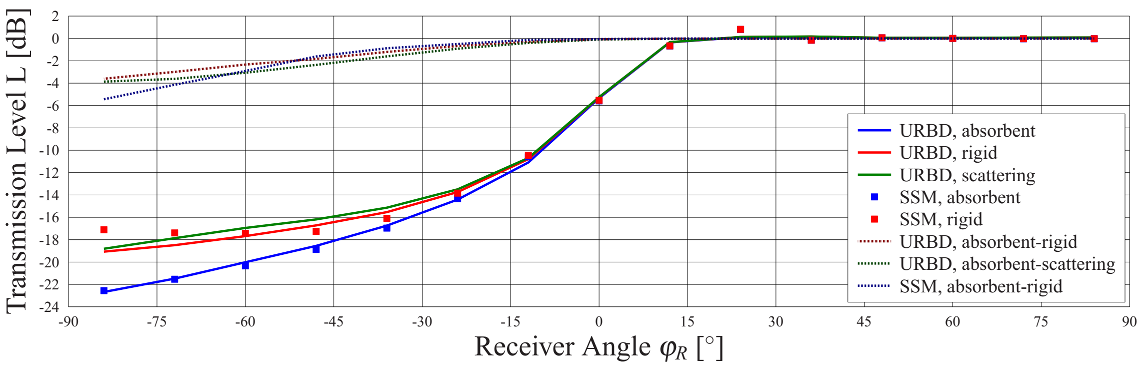

(B) Reflecting surface behind the wedge, either specular or diffuse.

FIGURE 2: Transmission level of reflecting surfaces.

That can be explained by the coherent addition of the SSM compared with the energetic one of the URBD.

Series 2: In the second simulation series, the reflection of the floor behind the wedge (region B) is altered and the front surface (region F) is absorbent (see Fig. 2b).

Shadow Zone: In contrast to the reflecting floor in front of the wedge, a reflecting surface behind the wedge increases the transmission level up to $3.7dB$ in the deep shadow in case of the URBD computations. This is caused by additionally detected diffracted sound particles, which are reflected by the floor behind the wedge. In case of a rigid surface, only reflected sound particles with larger diffraction angles – and thus less energy – can be detected. In contrast, in case of a scattering surface, $0.5dB$ higher transmission levels are observed as also sound particles with smaller diffraction angles (and thus higher energy) can be reflected to the receivers. Thus, the scattering surface can increase the transmission loss even by more than $\Delta L = 3dB$ for an energetic model. Due to coherent additions, the exact SSM yields higher increases in some cases, but it can be stated (see the Fig. 2): the agreement with the URBD is good except for the deep shadow case.

View Zone: The transmission level is independent of the surface type (absorbent, rigid and scattering surface) with the SSM as well as with the URBD.

Series 3: Finally, the absorbent nature of the surfaces in front and behind the wedge is changed simultaneously to reflective. The result is: the single effects described above simply add up (compare Tab. 1).

Experiment II: The Effect Of The Opening Angle Of The Wedge

In the second experiment, the reflections of the wedge faces rather than the reflecting floor are studied, whereby the inner wedge angle φ_W is varied. Consequently, the reflecting floor is removed. The special (and for the URBD crucial) case of a wedge of $\varphi_W = 180°$, i.e. a plane surface, is handled separately.

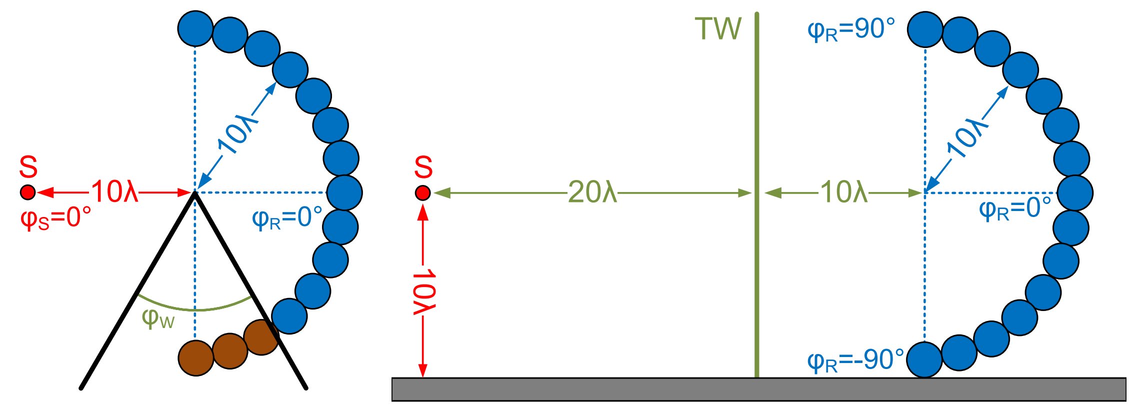

(A) Geometrical setup for the variation of the closed wedge angle. Invalid receivers are brown-colored.

(B) Geometrical setup for the extreme closed wedge angle of 180°.

FIGURE 3: Simulation setups.

Series 1: In the first simulation series, the wedge angle φ_W is varied in between $1° \leq \varphi_W \leq 150°$ in steps of 30° (see Fig. 3a). As the EDB is only capable of rigid surfaces forming an edge and the URBD is only influenced by their reflections, this series is restricted to rigid faces. The MDL is left out, because the detour is independent of the wedge angle. The results of the SSM and the URBD for different closed wedge angles φ_W are shown in Fig. 4a and Fig. 4b, respectively. A restriction is given as with increasing wedge angles impossible receiver positions arise (see Fig. 3a, brown-colored receivers). Only angles of $\varphi_R < -90° + \frac{\varphi_W}{2}$ are possible. In Fig. 4, additionally, zones of valid transmission levels for a given receiver angle φ_R, but different wedge angles φ_W, are indicated as a *pink band*.

Shadow Zone: The transmission level computed with the SSM strongly depends on the closed wedge angle φ_W. The transmission level increases for higher wedge angles φ_W up to $6dB$. This effect is due to the correct consideration of the boundary conditions in wave based diffraction theories. However, the combination of the URBD with the SPSM yields similar results than the SSM, although the URBD module is completely independent of the wedge angle. In contrast to the SSM, a maximum increase of $3dB$ is possible with the URBD due to the energetic addition of sound particles energies.

View Zone: In the view zone, the transmission level is constantly $0dB$ for all wedge angles below $\varphi_W \leq 90°$. Below this wedge angle, no sound energy can be reflected into the view zone, neither with SSM nor URBD. Starting from that wedge angle, sound energy is reflected into the view region and good agreements between SSM and URBD can be noticed. Due to interference effects, the SSM shows highly varying transmission levels for different receiver angles, whereas the URBD results in a smooth transmission level.

Series 2: In a second series, the transition of the wedge to a plane surface is looked at (see Fig. 3b). In case of the SSM, the diffraction impulse response vanishes for closed wedge angles $\varphi_W \rightarrow 180°$ automatically, such that the SSM results need not to be considered here. In case of the URBD, however, diffraction is computed for a $\varphi_W = 179°$ wedges, but not for $\varphi_W = 181°$

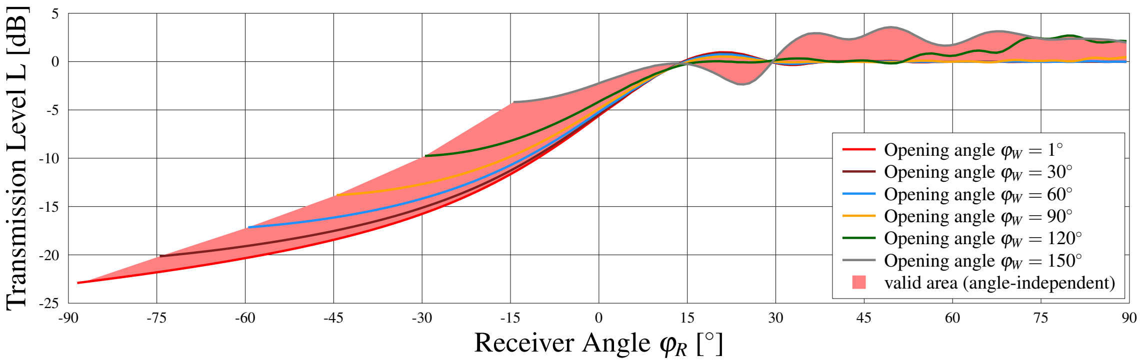

(A) Secondary Source model.

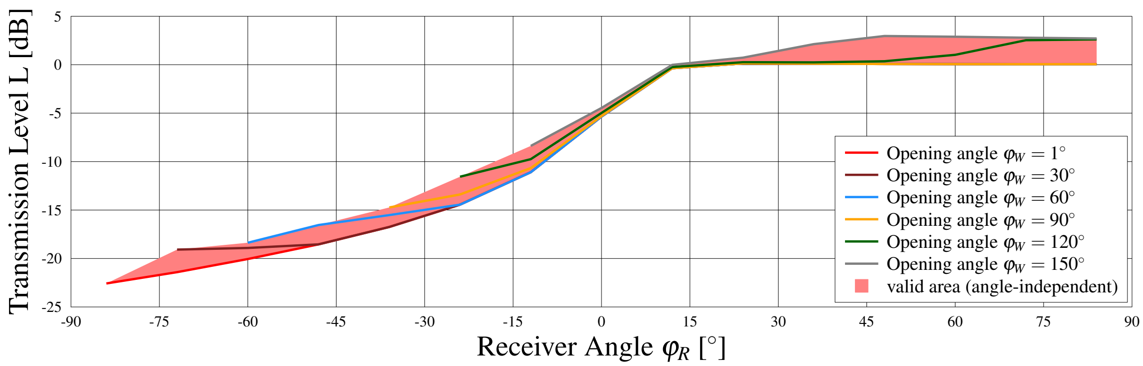

(B) Uncertainty Relation Based Diffraction.

FIGURE 4: Transmission level for different closed wedge angles φ_W.

wedges. To investigate this non-physical effect, a TW is placed upon a flat surface ($\varphi_W = 180°$). The flanking surfaces, being actually only one, are defined as either completely absorbing ($\alpha = 1.0$) or completely reflecting ($\alpha = 0.0$).

Totally absorbent flanking surfaces: The difference in the transmission level computed by URBD without diffraction (no TW) indeed equals the free-field transmission level of $0dB$ exactly. Very astonishingly for this absurd case, the introduction of a TW, and, thus, an artificial diffraction does almost not affect the transmission level (differences $< 0.1dB$). This may be explained as there is only a view zone here and most of the sound particles pass the *edge* in a large distance, i.e., are almost not deflected.

Rigid, totally reflecting flanking surfaces: As expected, the sound particle experiments yields a transmission level of almost $3dB$ for all receivers if no TW is present. Compared to that, the insertion of a TW causes a small increase of the transmission level ($0.2dB$) for all receivers except for the receivers around $|\varphi_R \leq 15°|$, where the transmission level decreases (up to $1dB$). This missing energy can be explained by the fact that sound particles, which are responsible for these receivers, are reflected on the floor close to the *foot* of the TW. These sound particles closely pass by the *edge* such that they are scattered over a wide angle range. The latter explains the slightly increased energy for the remaining receivers. Beside this artifact, the transmission degree is astonishingly only weakly influenced by the insertion of the artificial TW.

Conclusion and Outlook

The influence of the inner wedge angle and reflecting floors in front or behind the wedge on the transmission degree of edge diffraction were analyzed for the exact wave based SSM as well as for the URBD. Although the two are based on extremely different assumptions, the agreements are astonishingly very good, even in cases, where a failure of the URBD had been feared, especially in the 180°-wedge-case. The simple detour-model fails in some of these cases as expected. Only the URBD can handle rough instead of flat surfaces, but the influence of scattering is weak. After these investigations, it seems that, in spite of the quite rough assumptions of the simple URBD model, at least in many practical cases, this model is really generalizable for arbitrary combinations of higher order reflections and diffractions. The URBD as well as the SSM has to be validated for higher order reflections and diffractions in the future.

References

[1] U. M. Stephenson, "An energetic approach for the simulation of diffraction within ray tracing based on the uncertainty relation", Acta Acustica united with Acustica **96**, 516–535 (2010).

[2] A. Pohl and U. Stephenson, "From ray to beam tracing and diffraction - an analytical prognosis formula for the trade-off between accuracy and computation time", in *Proceedings of DAGA* (Berlin, Germany) (2010).

[3] D. Schröder, A. Pohl, U. P. Svensson, M. Vorländer, and U. Stephenson, "On the accuracy of edge diffraction simulation methods in geometrical acoustics", in *Proceedings of Internoise* (New York, U.S.A.) (2012).

[4] A. Pohl and U. Stephenson, "Efficient simulation of sound propagation including multiple diffractions in urban geometries by convex sub-division", in *Proceedings of Internoise* (Lisbon, Portugal) (2010).

[5] A. D. Pierce, *Acoustics: An Introduction to Its Physical Principles and Applications* (Acoustical Society of America) (1989).

[6] M. Born and E. Wolf, *Principles of Optics*, 7 edition (Cambridge University Press) (1999).

[7] U. J. Kurze, "Noise reduction by barriers", The Journal of the Acoustical Society of America **55**, 504–518 (1974).

[8] Z. Maekawa, "Noise reduction by screens", Applied Acoustics **1**, 157–173 (1968).

[9] H. Medwin, "Shadowing by finite noise barriers", The Journal of the Acoustical Society of America **69**, 1060–1064 (1981).

[10] U. P. Svensson, R. I. Fred, and J. Vanderkooy, "An analytic secondary source model of edge diffraction impulse responses", The Journal of the Acoustical Society of America **106**, 2331–2344 (1999).

[11] U. P. Svensson, "Edge Diffraction Matlab Toolbox, `www.iet.ntnu.no/ svensson/software/index.html`", (2010).

[12] U. M. Stephenson, "Introducing higher order diffraction into beam tracing based on the uncertainty relation", Building Acoustics **18**, 59–82 (2011).